Supporting Information

Rapid Quantitative Measurements of Paramagnetic Relaxation Enhancements in Cu(II)-Tagged Proteins by Proton-Detected Solid-State NMR Spectroscopy

*Dwaipayan Mukhopadhyay, Philippe S. Nadaud, Matthew D. Shannon, and Christopher P. Jaroniec**

Department of Chemistry and Biochemistry, The Ohio State University, Columbus, OH 43210

* E-mail: jaroniec.1@osu.edu

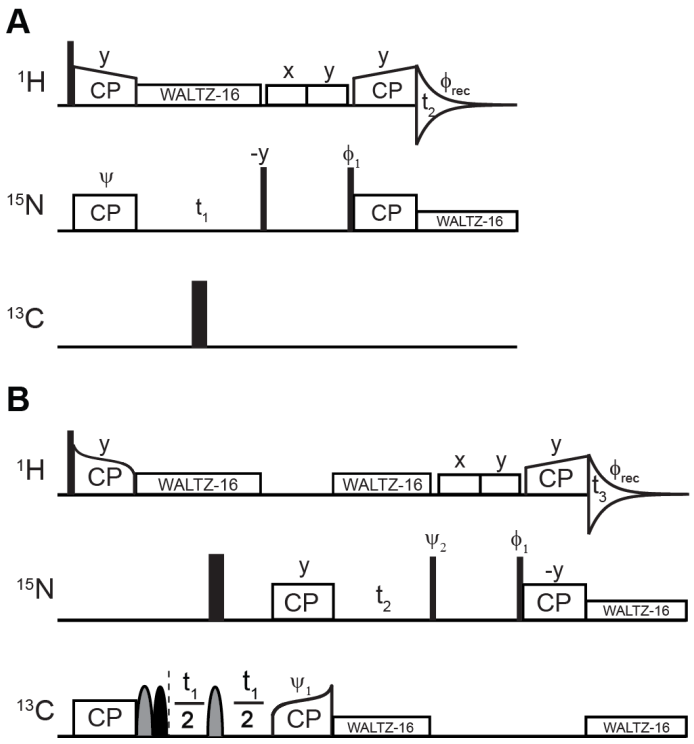

Figure S1. Pulse schemes for the **(A)** 2D ^{15}N-^{1}H and **(B)** 3D ^{13}CO-^{15}N-^{1}H experiments based on those of Barbet-Massin et al.[1] Narrow and wide black rectangles correspond to 90º and 180º pulses, and all pulses have phase *x* unless indicated otherwise. WALTZ-16 decoupling[2] at field strength of ~5 kHz was applied on the ^{1}H, ^{15}N and ^{13}C channels as indicated. Solvent suppression was achieved using a modified MISSISSIPI scheme,[3] consisting of alternating *x* and *y* pulses at 5 kHz field strength applied for a maximum period of 80 ms and decremented with increasing t_1 and t_2 to keep the duration constant for the entire pulse scheme. **(A)** Parameters used to record ^{15}N-^{1}H spectra at MAS rate of 60 kHz were as follows. The ^{1}H, ^{13}C, and ^{15}N carriers were placed at ~4.7, ~100 and ~120 ppm respectively. ^{1}H-^{15}N cross-polarization[4] was achieved using a ~15 kHz ^{15}N field, a linearly ramped ^{1}H field centered around ~75 kHz field strength, and a contact time of 1.5 ms. For the ^{15}N-^{1}H cross-polarization prior to ^{1}H signal detection a 720 μs contact time was used. The following minimal two-step phase cycle was employed: $\phi_1 = y, -y$; $\psi = x$; receiver = *y*, *-y*. Quadrature detection in the ^{15}N dimension was achieved by alternating phase ψ according to the States-TPPI method.[5] **(B)** Parameters used to record ^{13}CO-^{15}N-^{1}H spectra at MAS rate of 60 kHz were as follows. The ^{1}H, ^{13}C, and ^{15}N carriers were placed at ~4.7, ~175 and ~120 ppm respectively. A 15 kHz ^{13}C field and a ^{1}H field centered around ~75 kHz field strength applied with a tangent ramp, and a contact time of 2 ms were used to achieve ^{1}H-^{13}CO cross-polarization. ^{13}CO-^{13}Cα J-decoupling during ^{13}CO chemical shift evolution (t_1) was achieved by applying a 266.67 μs r-SNOB[6] selective ^{13}CO 180º pulse (filled black shape; applied on-resonance at ~175 ppm frequency) and selective ^{13}Cα 180º pulses (filled grey shapes; applied off-resonance at ~55 ppm frequency) as indicated. ^{13}CO-^{15}N SPECIFIC-CP[7] was employed with a ~ 25 kHz field on ^{13}C (tangent ramp), ~ 35 kHz field on ^{15}N, and a contact time of 9 ms. For the final ^{15}N-^{1}H magnetization transfer the CP conditions were same as in panel (A). The following minimal two-step phase cycle was employed: $\phi_1 = x, -x$; $\psi_1 = x$; $\psi_2 = x$, receiver = *y*, *-y*. Quadrature in the ^{13}C and ^{15}N dimensions was achieved by alternating phases ψ_1 and ψ_2 according to the States-TPPI method.

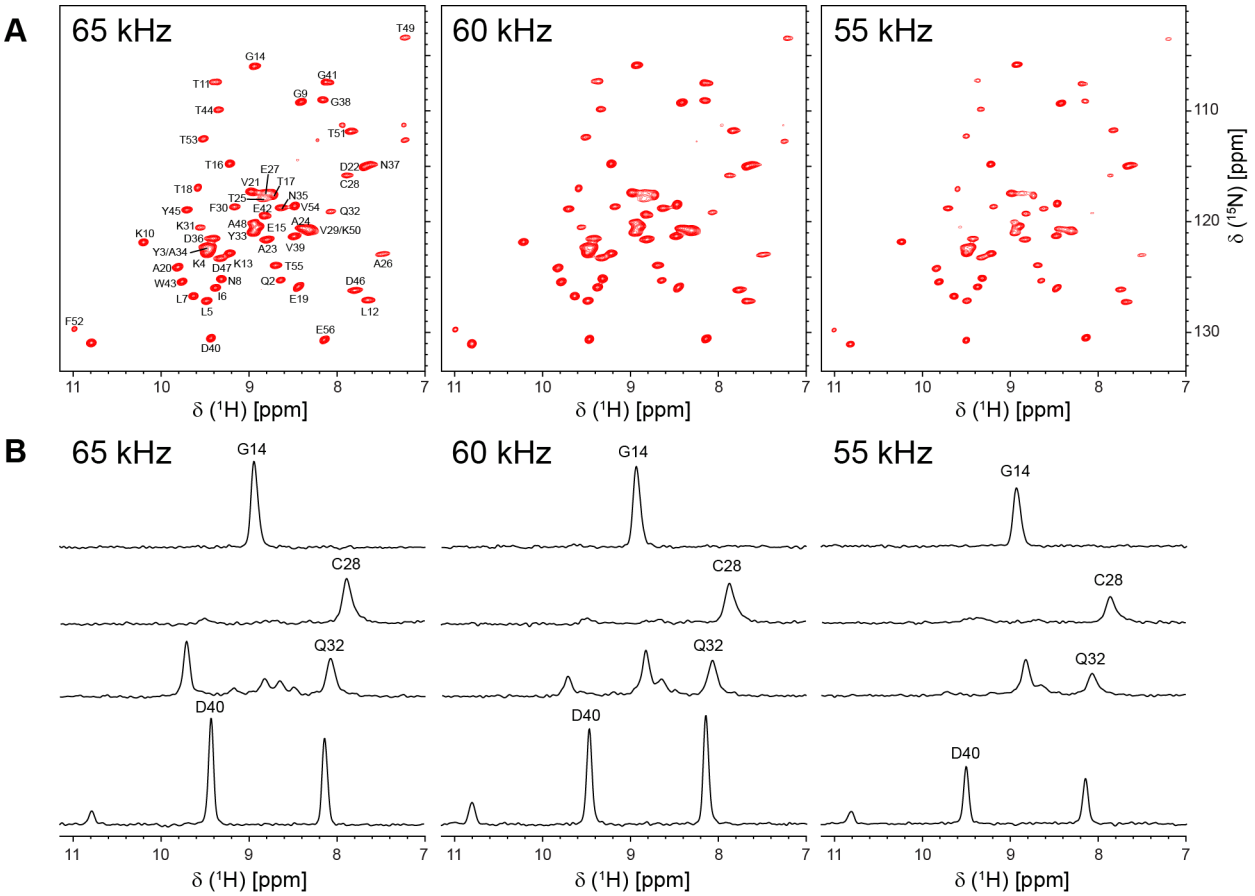

Figure S2. (A) 2D ^{15}N-^{1}H spectra and (**B**) representative slices corresponding to ^{15}N frequencies of residues G14, C28, Q32, and D40 for ^{2}H,^{13}C,^{15}N-labeled 28EDTA-Cu^{2+} back-exchanged with H_2O and diluted in a ~1:3 molar ratio in natural abundance GB1 as described in the text. The spectra were recorded using the pulse scheme in Figure S2 at 800 MHz ^{1}H frequency and MAS rates of 65, 60 and 55 kHz as indicated, with $t_{1,max}$ (^{15}N) = 25 ms, $t_{2,max}$ (^{1}H) = 30 ms, 2 scans per row and total measurement times of ~2.5 minutes. The spectra were processed with cosine-bell window functions in both dimensions and are shown with the first contour drawn at ~30 times the rms noise level. The average signal-to-noise ratios were found to be 100, 90, and 64 for MAS rates of 65 kHz, 60 kHz, and 55 kHz, respectively, and the average linewidths in the ^{1}H dimension were 63, 66 and 69 Hz for MAS rates of 65 kHz, 60 kHz, and 55 kHz, respectively.

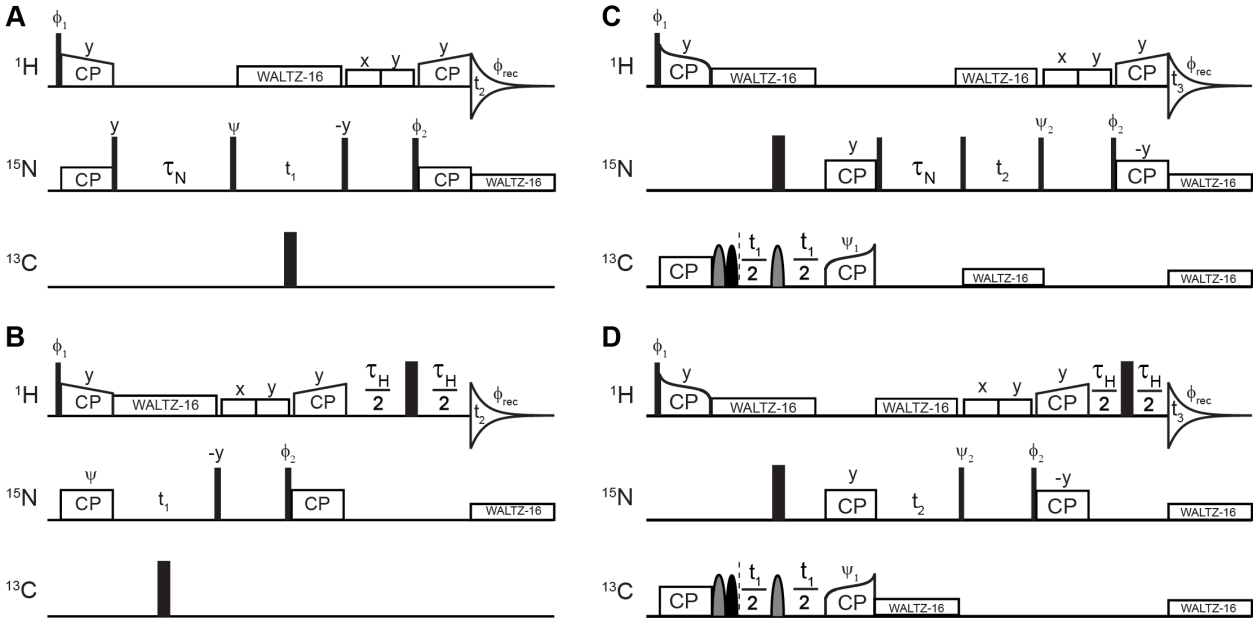

Figure S3. (A, B) 2D ^{15}N-^{1}H based pulse schemes for the site-specific measurement of backbone amide (**A**) ^{15}N longitudinal relaxation rate constants and (**B**) ^{1}H transverse relaxation rate constants. The experimental parameters used were the same as those listed in Figure S1A caption. The following minimum four-step phase cycle was employed: $\phi_1 = x, -x$; $\psi = -y$ in (**A**) and $\psi = x$ in (**B**); $\phi_2 = 2(y), 2(-y)$; receiver = $y, -y, -y, y$. Quadrature in the ^{15}N dimension was achieved by alternating phase ψ according to the States-TPPI method. **(C, D)** 3D ^{13}CO-^{15}N-^{1}H based pulse schemes for the site-specific measurement of backbone amide (**C**) ^{15}N longitudinal relaxation rate constants and (**D**) ^{1}H transverse relaxation rate constants. The experimental parameters used were the same as those listed in Figure S1B caption. The following minimum four-step phase cycle was employed: $\phi_1 = x, -x$; $\psi_1 = x$; $\psi_2 = x$; $\phi_2 = 2(x), 2(-x)$; receiver = $y, -y, -y, y$. Quadrature in the ^{13}C and ^{15}N dimensions was achieved by alternating phases ψ_1 and ψ_2 according to the States-TPPI method.

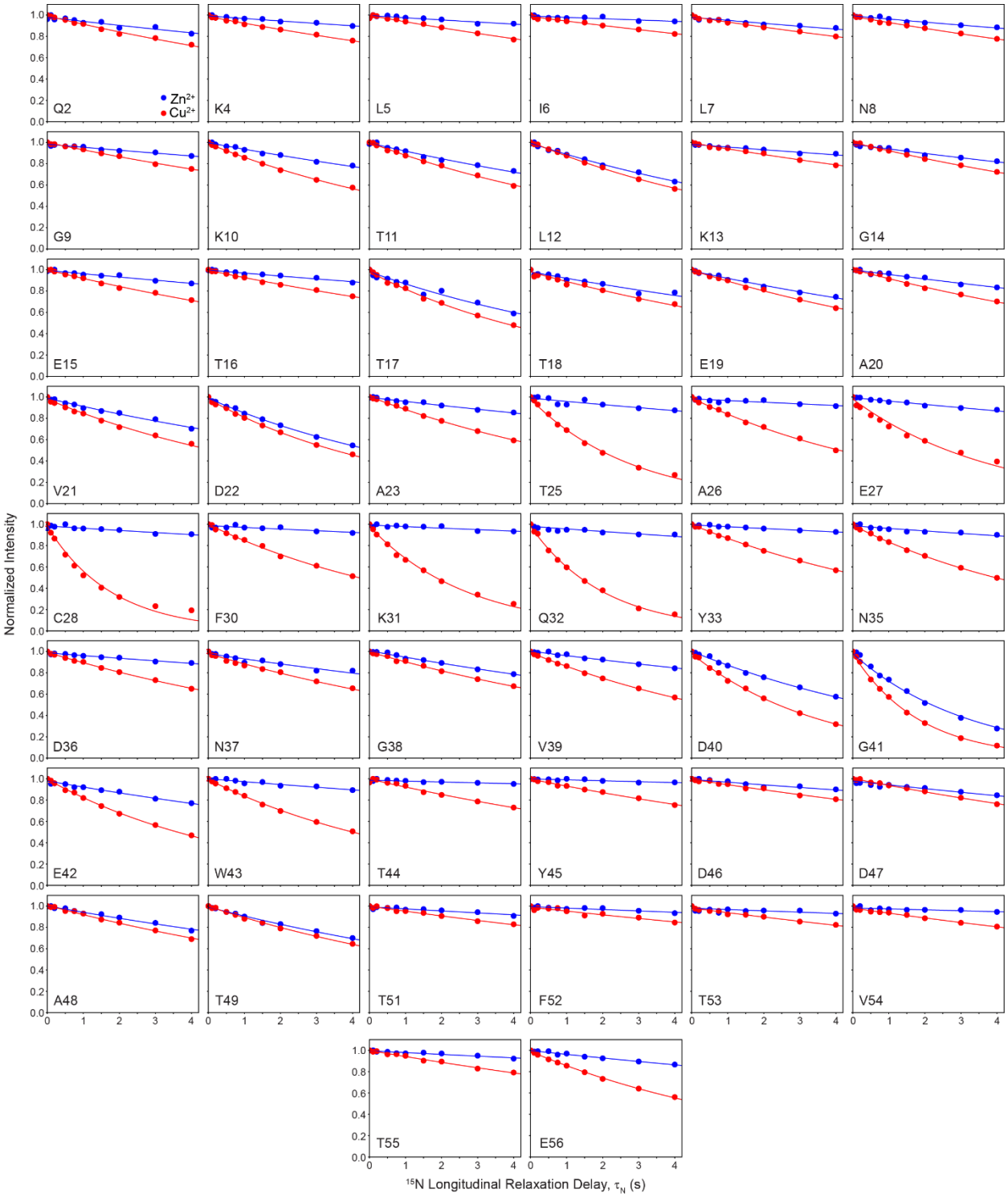

Figure S4. Residue-specific amide ^{15}N longitudinal relaxation trajectories measured from a series of 2D ^{15}N-^{1}H spectra recorded with different values of the delay τ_N (c.f., Figure S3A) for 28EDTA-Zn^{2+} (blue circles) and 28EDTA-Cu^{2+} (red circles). Best fits of the relaxation trajectories to decaying single exponentials are shown as lines of the corresponding color.

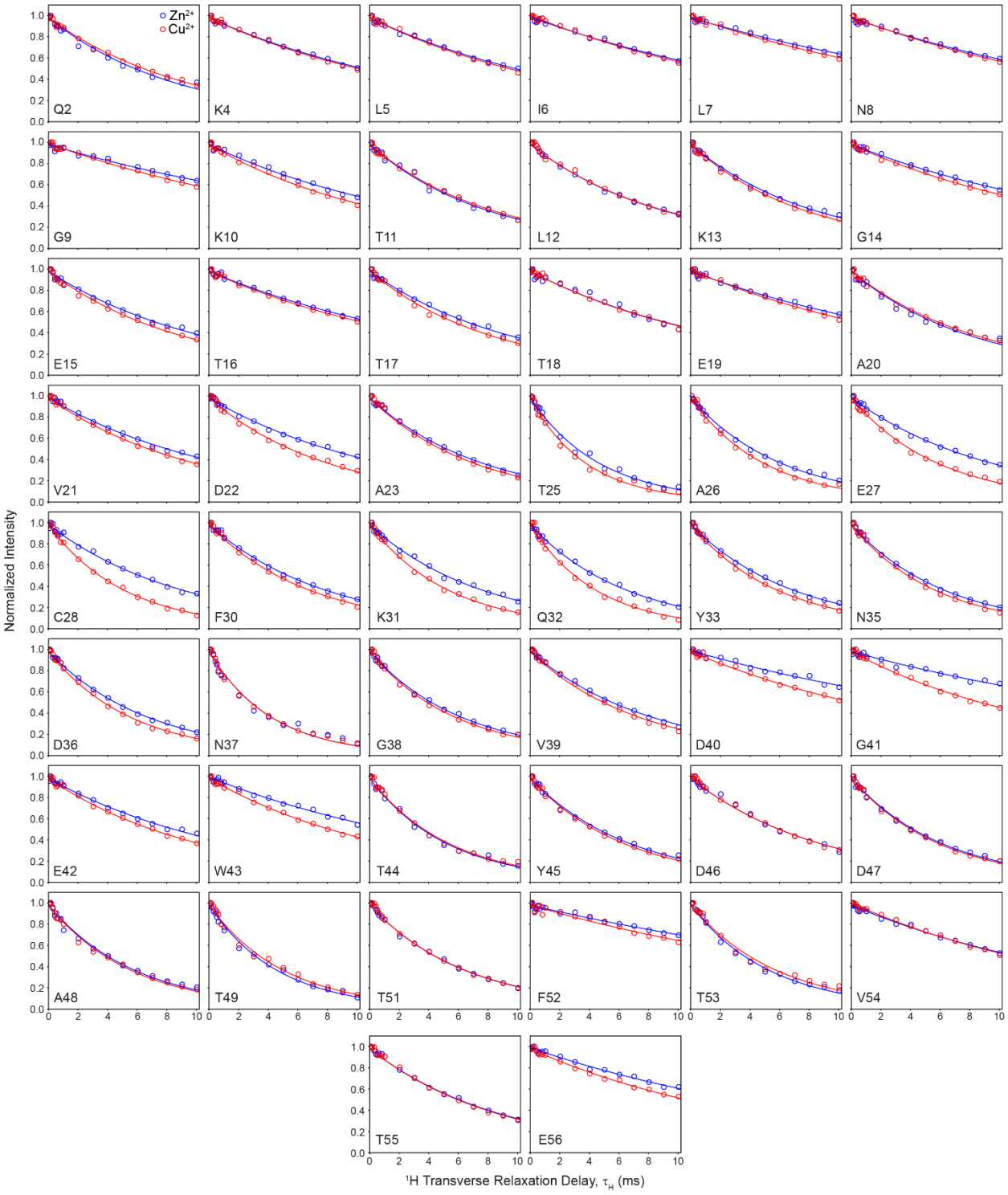

Figure S5. Residue-specific amide ^{1}H transverse relaxation trajectories measured from a series of 2D ^{15}N-^{1}H spectra recorded with different values of the delay τ_H (c.f., Figure S3B) for 28EDTA-Zn^{2+} (blue open circles) and 28EDTA-Cu^{2+} (red open circles). Best fits of the relaxation trajectories to decaying single exponentials are shown as lines of the corresponding color.

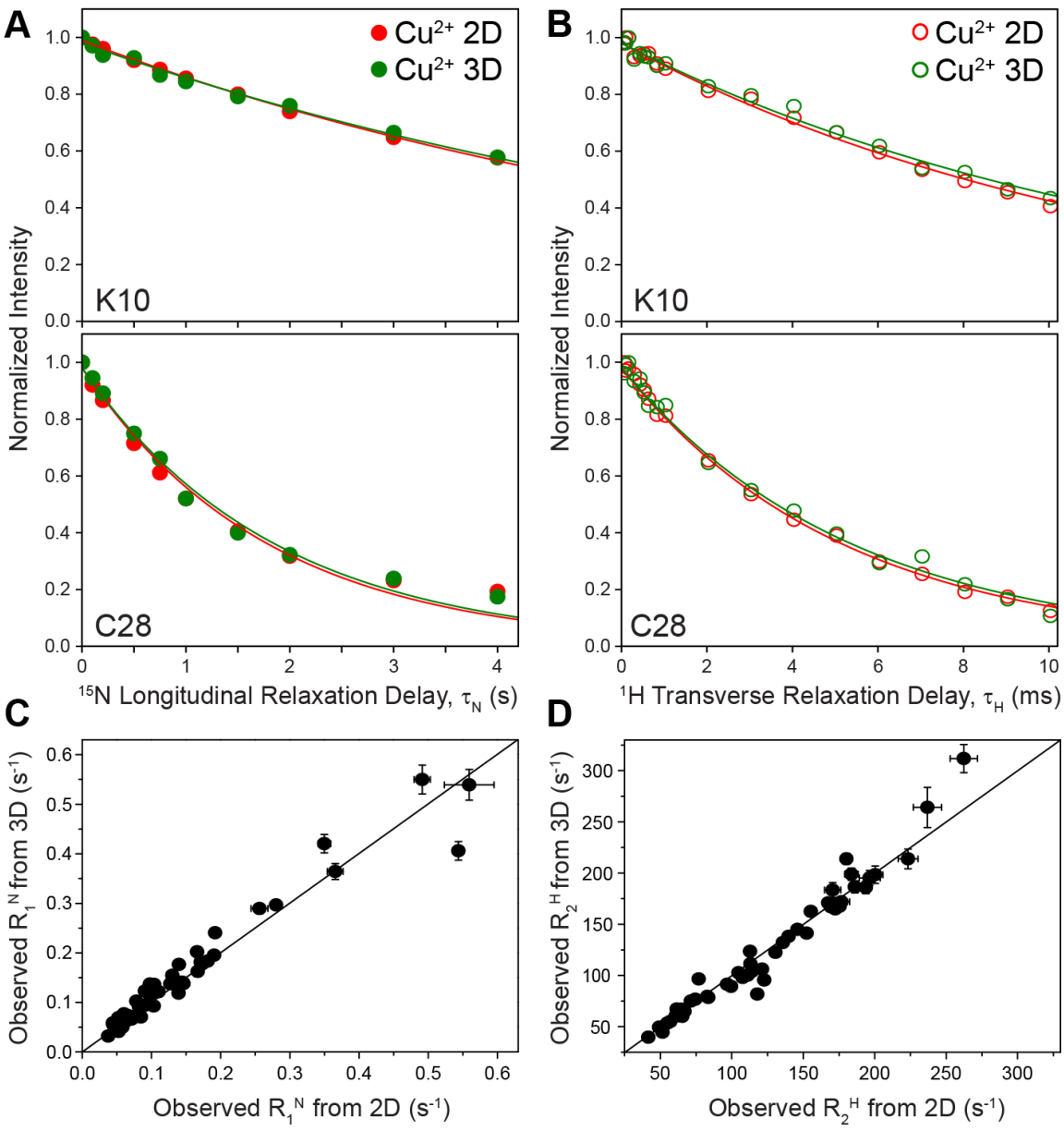

Figure S6. Representative amide ^{15}N R_1 (**A**) and ^{1}H R_2 (**B**) trajectories for residues K10 and C28 in 28EDTA-Cu^{2+} recorded using experiments based on a series of 2D ^{15}N-^{1}H spectra (red filled and open circles; c.f., pulse schemes in Figure S3A and S3B) and 3D ^{13}CO-^{15}N-^{1}H spectra (green filled and open circles; c.f., pulse schemes in Figure S3C and S3D). Best fits of the relaxation trajectories to decaying single exponentials are shown as lines of the corresponding color. (**C, D**) Correlation plots for the experimental ^{15}N R_1 (**C**) and ^{1}H R_2 (**D**) rates determined via series of 2D ^{15}N-^{1}H spectra versus series of 3D ^{13}CO-^{15}N-^{1}H spectra.

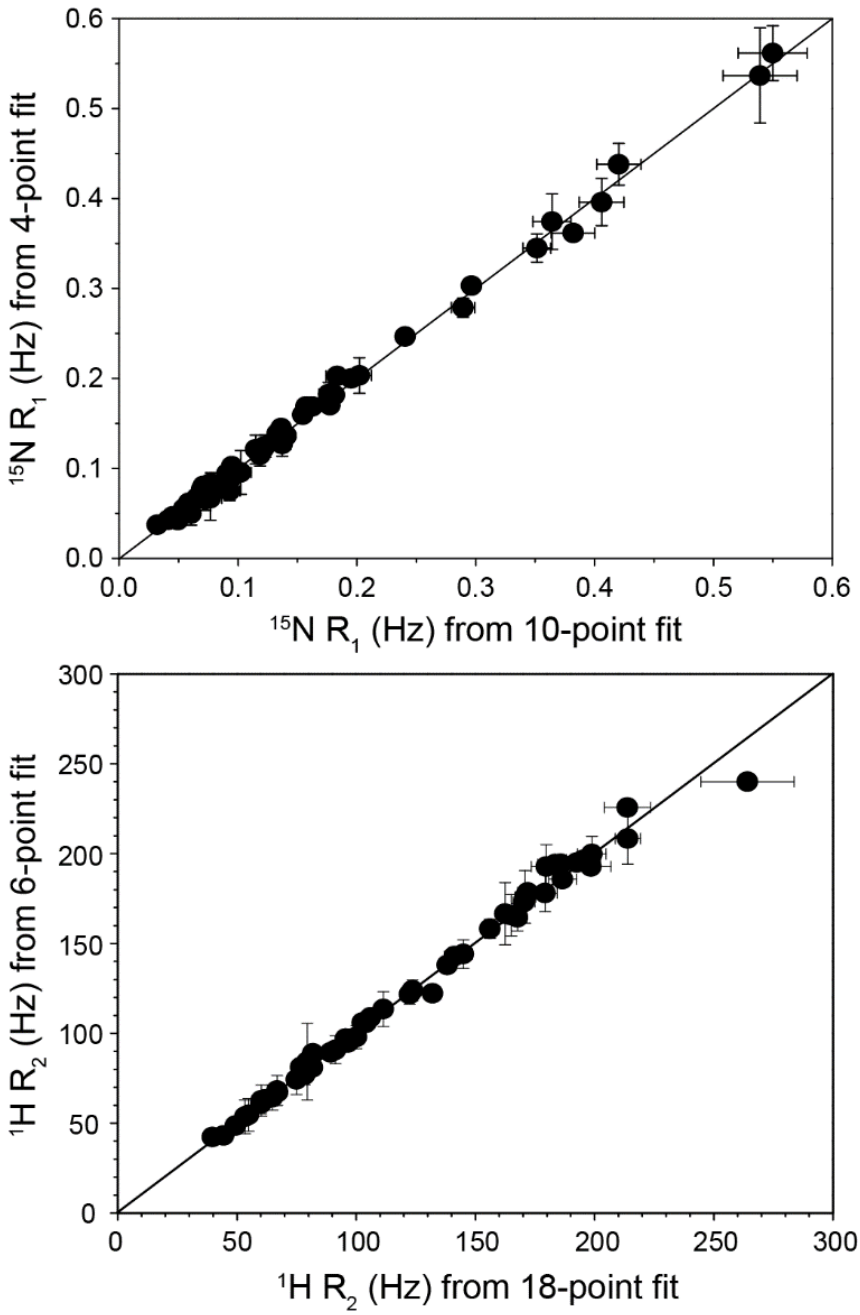

Figure S7. Correlation plots for the experimental amide ^{15}N R_1 (top) and ^{1}H R_2 (bottom) rates extracted from complete relaxation trajectories determined using a series of 10 and 18 3D ^{13}CO-^{15}N-^{1}H spectra for ^{15}N R_1 and ^{1}H R_2, respectively (c.f., Figures S4 and S5), versus the corresponding values determined from sparse trajectories consisting of four (τ_N values of 100 μs, 0.5 s, 1.5 s, and 3 s) and six (τ_H values of 66.7 μs, 633.3 μs, 2.0333 ms, 4.0333 ms, 8.0333 ms and 10.0333 ms) points in the relaxation dimension for ^{15}N R_1 and ^{1}H R_2, respectively.

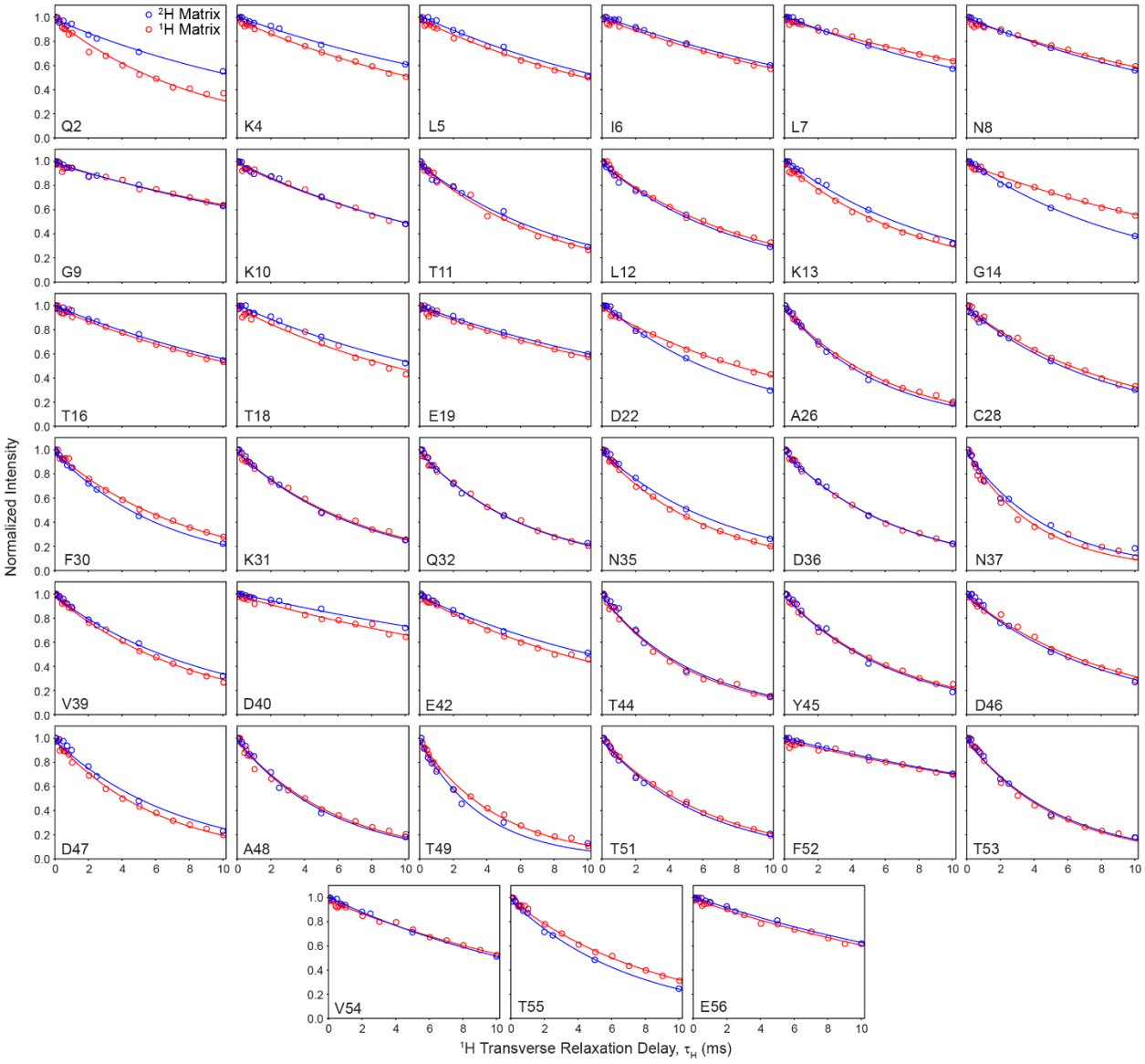

Figure S8. Residue-specific amide ^{1}H transverse relaxation trajectories measured at 800 MHz ^{1}H frequency and 60 kHz MAS rate from series of 2D ^{15}N-^{1}H spectra for ^{2}H,^{13}C,^{15}N-labeled diamagnetic GB1 analogs diluted in a ~1:3 molar ratio in ^{2}H-GB1 (blue circles) or natural abundance (^{1}H) GB1 (red circles) and back-exchanged with 100% H_2O. Best fits of the relaxation trajectories to decaying single exponentials are shown as lines of the corresponding color.

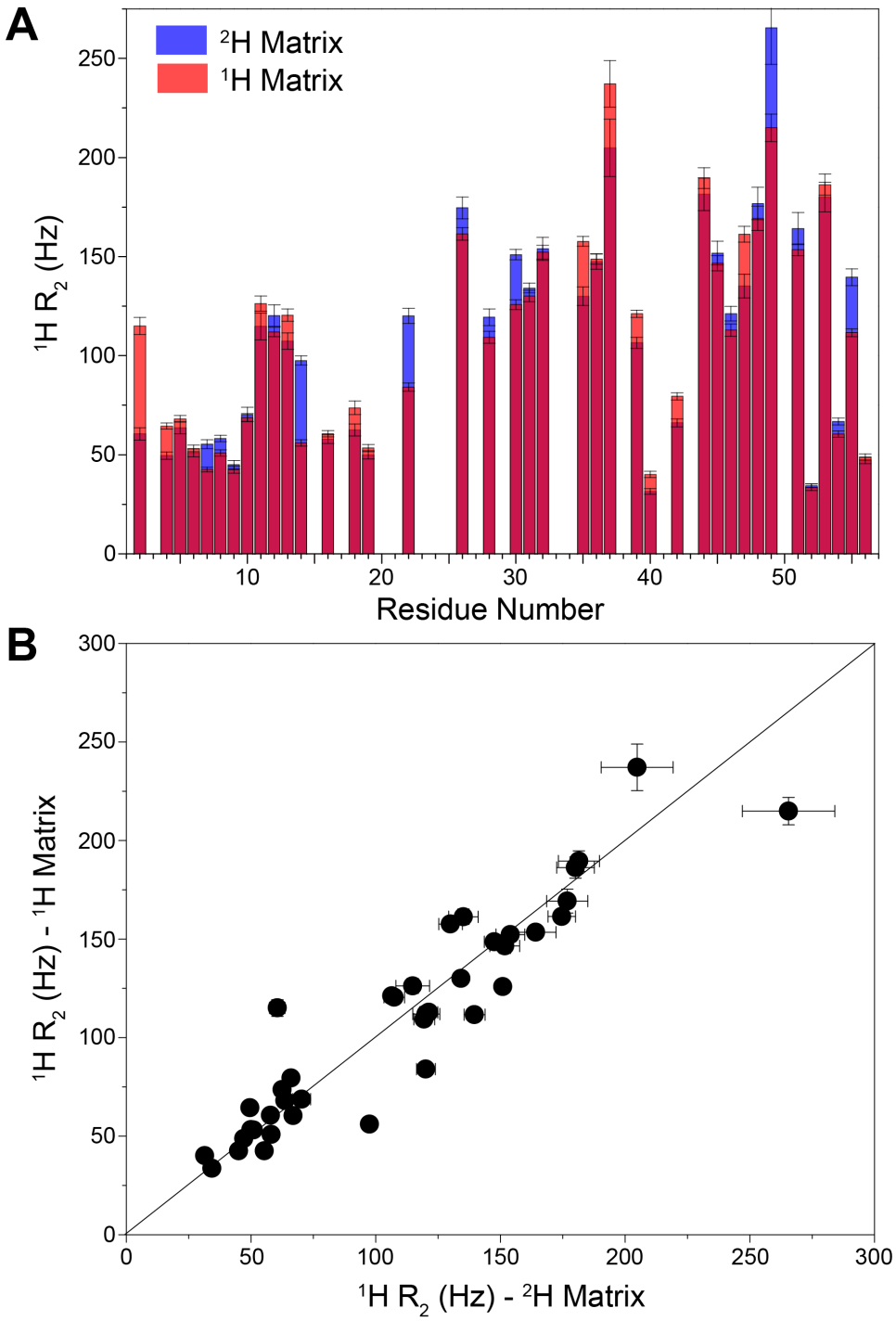

Figure S9. (**A**) Residue-specific amide ^{1}H R_2 rate constants as a function of residue number extracted from the trajectories shown in Figure S8 for ^{2}H,^{13}C,^{15}N-labeled proteins diluted in a matrix of ^{2}H-labeled GB1 and natural abundance (^{1}H) GB1. The average ^{1}H R_2 rates were found to be 109 ± 54 and 109 ± 53 for the ^{2}H and ^{1}H matrices, respectively. (**B**) Correlation plot for the amide ^{1}H R_2 rate constants determined for the ^{2}H and ^{1}H matrices. The R^2 value was found to be 0.88.

Supporting Information References

(1) Barbet-Massin, E.; Pell, A. J.; Retel, J. S.; Andreas, L. B.; Jaudzems, K.; Franks, W. T.; Nieuwkoop, A. J.; Hiller, M.; Higman, V.; Guerry, P.; Bertarello, A.; Knight, M. J.; Felletti, M.; Le Marchand, T.; Kotelovica, S.; Akopjana, I.; Tars, K.; Stoppini, M.; Bellotti, V.; Bolognesi, M.; Ricagno, S.; Chou, J. J.; Griffin, R. G.; Oschkinat, H.; Lesage, A.; Emsley, L.; Herrmann, T.; Pintacuda, G., Rapid proton-detected NMR assignment for proteins with fast magic angle spinning. *J. Am. Chem. Soc.* **2014,** *136*, 12489-12497.

(2) Shaka, A. J.; Keeler, J.; Freeman, R., Evaluation of a new broadband decoupling sequence: WALTZ-16. *J. Magn. Reson.* **1983,** *53*, 313-340.

(3) Zhou, D. H.; Rienstra, C. M., High-performance solvent suppression for proton detected solid-state NMR. *J. Magn. Reson.* **2008,** *192*, 167-172.

(4) Pines, A.; Gibby, M. G.; Waugh, J. S., Proton-enhanced NMR of dilute spins in solids. *J. Chem. Phys.* **1973,** *59*, 569-590.

(5) Marion, D.; Ikura, M.; Tschudin, R.; Bax, A., Rapid recording of 2D NMR spectra without phase cycling. Application to the study of hydrogen exchange in proteins. *J. Magn. Reson.* **1989,** *85*, 393-399.

(6) Kupce, E.; Boyd, J.; Campbell, I. D., Short selective pulses for biochemical applications. *J. Magn. Reson. B* **1995,** *106*, 300-303.

(7) Baldus, M.; Petkova, A. T.; Herzfeld, J.; Griffin, R. G., Cross polarization in the tilted frame: assignment and spectral simplification in heteronuclear spin systems. *Mol. Phys.* **1998,** *95*, 1197-1207.